

## EXPERIMENTAL STUDY ON GREEN AND GRAY INFRASTRUCTURE EFFECTS ON OVERTOPPING

JORDAN KECK<sup>1</sup>, TORI TOMICZEK<sup>2</sup>, DAN McMANN<sup>3</sup>, DANIEL COX<sup>4</sup>, MAGARET LIBBY<sup>5</sup>, PEDRO LOMONACO<sup>6</sup>

1 USNA, USA, [m243222@usna.edu](mailto:m243222@usna.edu) 2 USNA, USA, [vjohsnon@usna.edu](mailto:vjohsnon@usna.edu) 3 USNA, USA, [m244176@usna.edu](mailto:m244176@usna.edu)

4 OSU, USA, [dan.cox@oregonstate.edu](mailto:dan.cox@oregonstate.edu) 5 OSU, USA, [libbym@oregonstate.edu](mailto:libbym@oregonstate.edu) 6 OSU, USA, [pedro.lomonaco@oregonstate.edu](mailto:pedro.lomonaco@oregonstate.edu)

### ABSTRACT

This paper presents results of a reduced (1:8) scale experiment investigating the performance of hybrid structural (gray) and natural-based (green) infrastructure for wave overtopping reduction. Experiments were scaled to a 1:8 geometric scale based on 1:2-scale experiments conducted during the Summer of 2023 at Oregon State University. Seven wave conditions were tested, with (model-scale) wave periods ranging from 1 to 2 seconds and wave heights ranging from 6.0 to 7.5 cm. These wave conditions were conducted throughout two configurations: a seawall-only (baseline) configuration and a configuration with the seawall in combination with a mangrove forest installed seaward of the wall. The total volume of overtopped water was measured for each wave condition. Results indicated that adding mangroves reduced overtopping for all wave conditions, with an average of 32.1% reduction in overtopped volume compared to the baseline configurations. This reduction falls within the range of preexisting overtopping rates. Results from these experiments can assist engineers in understanding the performance of hybrid coastal infrastructure to design effective and sustainable shoreline protection.

**KEYWORDS:** Physical model experiment, overtopping, *Rhizophora mangle*, hybrid infrastructure, coastal resilience

### INTRODUCTION

Coastal communities face numerous coastal hazards that are increasing with climate change (sea level rise, unpredictable weather events, frequent flooding), making shore protection systems vital to mitigate impacts to near shore infrastructure and populations. For example, wave overtopping, which is experienced among coasts throughout the world, can damage infrastructure and create unsafe driving conditions on nearshore roadways. An example is shown in Figure 1, where waves in Annapolis, MD overtop a local roadway stabilized by a rip rap revetment during a coastal flooding event. Vulnerability to these natural hazards and risks to human life and infrastructure may increase in future decades. Hence, coastal protection solutions must be practical, sustainable, and adaptable to future conditions. Recently, there has been a rise in the combination of green/hybrid solutions to coastal protection, but effects of natural systems on reducing wave overtopping is uncertain.

Various types of coastal protection systems are utilized in shorelines throughout the world, and these systems range from conventional, structural solutions (gray) to natural and nature-based infrastructure (green). While there is growing interest in green and hybrid systems to mitigate wave overtopping, particularly to extend the design life of existing seawalls and revetments, there is a general lack of understanding of their engineering performance and the individual and combined effects of the green and gray components. In order to be able to employ nature-based coastal protection systems effectively, there must be more sophisticated engineering guidelines that are able to be cross referenced during the design process of coastal defenses (Ostrow et al., 2022).



**Figure 1: Waves Overtopping Roadway Stabilized by Rip Rap Revetment in Annapolis, MD**

Depending on geographic location, native vegetation can be incorporated with gray structures in order to provide coastal protection, which benefits the ecosystem along with providing reliable engineering performance. Common vegetation types that can be found as natural protection are seagrass, sea oats, panic grass, cordgrass, and mangroves, which are considered in this study. There are various species of mangroves, which vary in height, stem density, and salinity level tolerance. Mangroves are bound by climate requirements, where they are found in subtropical and tropical environments and can thrive in saline and brackish waters. The forests are bound by the latitudes of 25 degrees north and 25 degrees south; however, the majority of forests are found in the 5-degree upper and lower limits. Geographically, mangrove forests can be located along 118 countries' coastlines, with high forest densities located in The Philippines, Australia, Cuba and Florida (Verhagen, 2018).

Mangroves are classified as a valuable coastal habitat. The plants are capable of protecting the coast by dissipating waves and storm surge, storing carbon, and nurturing ecological diversity by providing shelter as marine nurseries (Alongi 2008). The plants also stabilize the coast by gathering sediment and reducing erosion (Menéndez et al., 2020). The genus of mangroves that is in focus throughout these experiments is a *Rhizophora* mangrove forest, in which trees create a dense network of above-ground prop roots. These forests serve as a first line of defense against natural hazards and protect coastal regions during extreme weather events such as tropical storms and tsunamis, and they can also mitigate erosion and wave heights during chronic wave conditions (Alongi 2008, Menéndez et al., 2020). The wave attenuation and water velocity reduction occur when water surges through the forest and the root system, where trunks and roots obstruct the water flow. Dense root systems help reduce erosion by fostering the deposition of sediments, which causes an increase in the thickness and richness of the soil within the forest. Mangroves can be coupled with conventional infrastructure such as seawalls and revetments to increase the effectiveness of coastal protection. To understand the effect of green and hybrid coastal protection on roadway overtopping mitigation, large- (1:2) and small- (1:8) scale experiments were performed to measure overtopping volumes under a range of incident wave conditions and experimental configurations. The reproduction of experiments at multiple scales further allows for scaling effects from reduced- to prototype scale to be assessed.

#### LARGE SCALE PHYSICAL MODEL

Large-scale (1:2) experiments were conducted at the Oregon State University Wave Research Laboratory throughout the summer of 2023 to measure the effects of mangroves on reducing overtopping of a coastal bulkhead or revetment (Libby et al. 2024). A 1-m wide tin tray filtered overtopped waves into a basin with load cells underneath to quantify the amount of water collected in the basin. Pumps were installed at the base of the flume to achieve a relatively constant water elevation during experiments. Random, regular, and transient wave conditions were tested with varying wave heights and periods resembling conditions ranging from typical daily conditions to extreme storm events. Multiple experimental configurations were implemented, including no mangrove forest and three forest densities seaward either a seawall alone, or a seawall fronted by a rubble mound revetment. All different configurations resulted in varying amounts of overtopping volume collected in the basin (Libby et al., 2024), with the highest density mangroves significantly reducing the overtopping volume. Fig. 2 shows the configurations from experiments by Libby et al. (2024) that will be compared with data collected in reduced-scale experiments at USNA: (1) seawall with no mangroves (baseline) (Fig. 2a), and (2) seawall with medium-density mangroves (1.61 trees/m<sup>2</sup> model scale / 0.40 trees/m<sup>2</sup> full scale) (Fig. 2b).



Figure 2: 1:2 Overtopping Experiments by Libby et al. (2024): (a) Baseline configuration (seawall, no mangroves); (b) mid-density mangrove forest configuration.

## REDUCED-SCALE PHYSICAL MODEL

### WAVE CONDITIONS

Experiments were conducted at the United States Naval Academy (USNA) in fall of 2023 and winter/spring of 2024. These tests further investigated the overtopping performance of mangrove forests by replicating the experiments performed by Libby et al. (2024) at a 1:8 geometric scale. The goal is to correlate various wave conditions, as shown in Table 1, with the quantified overtopping comparable to the experiments by Libby et al. (2024).

Table 1: Wave Conditions

Wave Condition	1:1 Prototype		1:2 Libby et al. (2024)		1:8 USNA (This Study)	
	H (cm)	T (s)	H (cm)	T (s)	H (cm)	T (s)
1*	48	2.8	24	2	6.0	1
2*	54	2.8	27	2	6.8	1
3*	60	2.8	30	2	7.5	1
4	48	4.2	24	3	6.0	1.5
5	54	4.2	27	3	6.8	1.5
6	60	4.2	30	3	7.5	1.5
7	48	5.7	24	4	6.0	2

\* Not tested by Libby et al. (2024)

Select wave conditions from Table 1 were unable to be conducted throughout overtopping due to the collection basin restraints. The waves with greater incident wave heights and longer periods resulted in larger waves, which caused more overtopping. The system was constrained by only being able to collect 6.8 kg of water due to the size of the collection basin. Each wave condition was tested in the baseline and seawall + mangrove configuration, besides Wave Condition 6, which was only able to be tested in the seawall + mangrove configuration because there was an excess of overtopping in the baseline configuration.

### 1.1 Materials and Methods

In order to construct the 1:8 model, a multitude of factors were considered during the design process. The most prominent design factors were cost, feasibility and size constraints. Experiments were conducted in the Coastal Basin in the United States Naval Academy's Hydromechanics Laboratory. A 0.61 m wide flume was placed within the middle of the basin, located 3.2 m from the wavemaker. The baseline configuration, depicted in Figure 3, consisted of no mangrove forest. The flume's bathymetry consisted of a 3.05 m long 1:20 slope leading to a flat portion where the mangrove forest was installed. The bathymetry was constructed by placing a wooden board which was designed to the size constraints of the flume and

existing bathymetry slope. The wooden slab also served as the stabilization for the mangrove roots where holes were drilled at preset distances based on the scaled dimensions. The roots were secured by placing them into the drilled holes, as the installation is shown in Figure 4.



Figure 3: Overview of Baseline Configuration



Figure 4: Installation of 1:8-Scale Mangrove Forest

In order to collect the overtopped volume, a collection basin was deployed behind the wall structure, which was 22 cm tall as shown in Figure 5. To secure the collection basin to the wall, c-clamps were utilized to prevent waves and water pressure from moving the collection basin from the wall. Additionally, a total of 15.9 kg of weights were placed in the bottom of the collection basin to act as a counterforce from the buoyancy caused by the surrounding water pressure.

The slit in the plastic of the basin was custom cut to a width of 0.29 m with a height which aligned with the height of the dam. To prevent reflected waves from reentering the end of the flume and splashing into the collection basin, regular waves were run in groups of either five or ten, depending on the wavelength, to achieve a total of 50 waves per wave condition.



Figure 5: Wall and Overtopping Basin for 1:8-scale Experiments

The schematic of the experimental set up of the seawall + mangrove configuration is depicted in Figure 6. In the figure, the brown wall represents a seawall or bulkhead structure. Experiments considered an offshore water depth of 41 cm, giving a water depth within the forest of 19 cm and a freeboard at the wall of 2.25 cm, scaled from that freeboard considered by Libby et al. (2024).

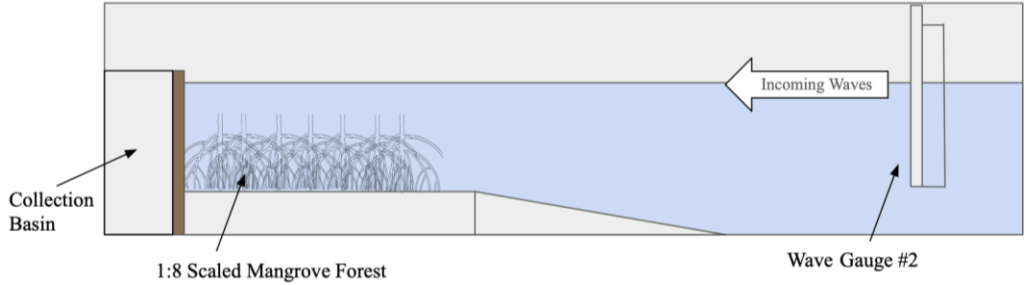


**Figure 6: Schematic of Experimental Configuration**

## 1.2 Results

Throughout each trial water was collected in the basin from waves overtopping the dam. This overtopping process is shown in Figure 7. Once a wave group of either five or ten waves were completed, the collection basin was removed from the coastal basin and weighed on a scale. Upon weighing, the basin was reinstalled into the flume and the next iteration of testing commenced once the water in the basin was still. Overtopped water weight was converted to volume based on assumed water density.



**Figure 7: Waves Overtopping the Wall into the Collection Basin during Baseline Condition**

Each wave condition was tested in the baseline and seawall + mangrove configuration, besides Wave Condition 6, which was only able to be tested in the seawall + mangrove configuration because there was an excess of overtopping in the baseline configuration. In order to calculate the normalized overtopped volume, Equation 1 was utilized, where  $Q$  represents the normalized overtopped volume,  $M_{water}$  is the mass of water (kg), and  $w_{slit}$  is the width of the slit (m).

$$Q = \frac{(M_{water}/\rho_{water})}{w_{slit}} \quad (m^3/m) \quad (1)$$

The normalized overtopped volume totals for each wave group were calculated and plotted in Figure 8. The filled in green shapes represent the conditions with the mangrove forest, whereas the blue outline shapes represent the baseline configuration. Each shape represents a different wave period, where the circles indicate 1-second wave periods, triangles represent 1.5-second wave periods and the square denotes the 2-second wave period for the wave conditions tested.

As shown in Figure 8, as both wave height and period increase, the amount of overtopped volume ( $Q$ ) also increases. The overtopped volume for the baseline configuration was represented by  $Q_b$  and the mangrove configuration ( $Q_m$ ). In addition, for any given wave condition, mangroves reduce the total amount of overtopping compared to the baseline configuration. Using Equation 2, percent reduction of normalized overtopped volume ( $Q$ ) was calculated between configurations, and results are plotted against wave height in Fig. 9. The shapes in Figure 9 correlate to the same wave periods as Figure 8.

$$\text{Percent Reduction} = \left( \frac{Q_b - Q_m}{Q_b} \right) \cdot 100\% \quad (2)$$

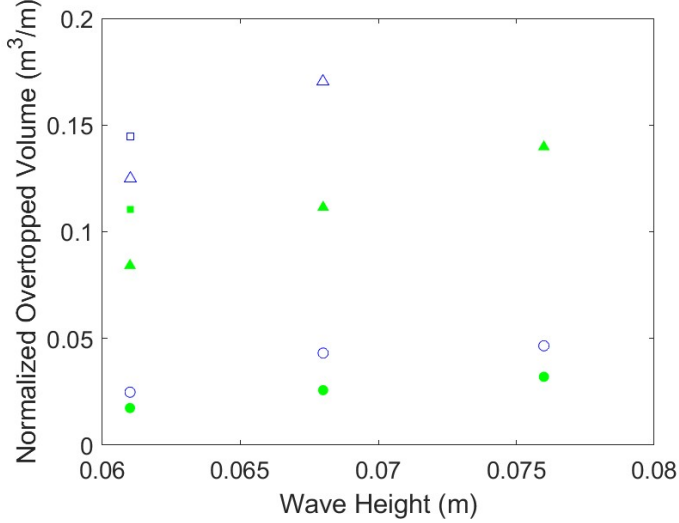


**Figure 8: Normalized Overtopped Volume per Unit Width ( $Q$ ) ( $m^3/m$ ) vs. Incident Wave Height ( $H$ ) (m).** Filled green shapes and hollow blue shapes indicate seawall + mangrove and baseline (no mangrove) configurations, respectively, while squares, triangles, and circles indicate 2 s, 1.5 s, and 1 s wave periods, respectively.

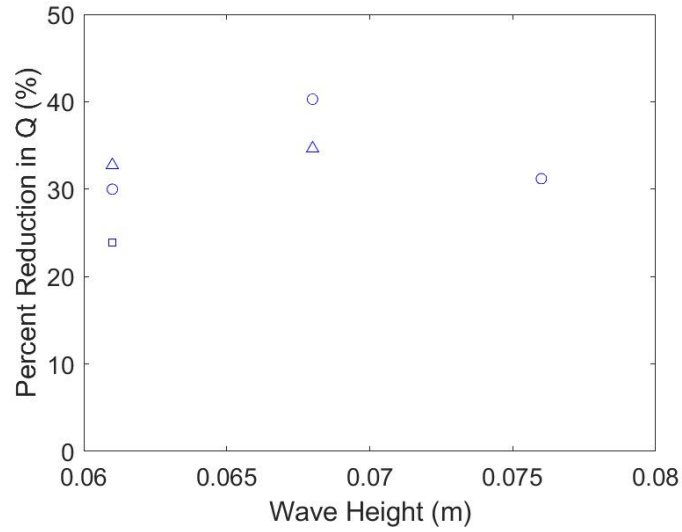


**Figure 9: Wave Height (m) versus Percent Reduction in  $Q$  (%)**

The average percent reduction in overtopping for the seawall + mangrove forest configuration compared to the baseline configuration across all the wave conditions was 32.1%. This average reduction percentage falls within the range of mangrove forests in nature, which are reported to cause a 13-66% reduction in overtopping (Verhagen and Loi, 2012). While additional tests are needed to determine any effects of the varying wave height ( $H$ ) and period ( $T$ ), in general, the 1 s and 1.5 s waves experienced a similar range of reduction, whereas the 2 s wave resulted in the mangroves having less of an effect on overtopping reduction. This result suggests that mangroves may be more effective at reducing overtopping for shorter-period wave conditions.

### 1.3 CONCLUSIONS

This study presented results of a reduced-scale physical model examination of the effects of mangrove forests on overtopping reduction. Scaling the experiments presented here based on tests performed at larger scale (Libby et al., 2024) provides an opportunity to further understand scaling effects of reduced-scale studies. This understanding is essential for accurate interpretation of results. More robust scaling relationships will allow facilities to conduct experiments when near-prototype scale experiments are not feasible. Overall, the experiments conducted in January of 2024 produced feasible overtopped volume results which fall within the ranges of preexisting overtopping reduction rates. Adding mangroves reduced

overtopping by 23.9% to 40.3%, with an average of 32.1% reduction compared to overtopping during the baseline condition. The presentation will describe the 1:8 experiments and results as well as future work focusing on comparing measured total overtopping volumes from reduced-scale tests with results from large-scale experiments by Libby et al. (2024).

## ACKNOWLEDGEMENT

A special thank you to the following individuals EN420 (Coastal Engineering Fall, 2024 class), Brandon Giginilliat, Mr. Pullen, Project Support Branch, and the Hydrolab Staff.

This project was supported by funding from NSF Grants 2037914, 2110262, 2110439, and 2129782 and the US Army Corps of Engineers through project number W912HZ2120045. Any opinions, findings, conclusions, or recommendations expressed in this material are those of the authors and do not necessarily reflect the views of the National Science Foundation, US Army Corps of Engineers, or US Naval Academy.

## REFERENCES

Alongi, D.M. (2008). Mangrove forests: Resilience, protection from tsunamis, and responses to global climate change. *Estuarine, Coastal and Shelf Science*. 76 (1). doi: 10.1016/j.ecss.2007.08.024

Libby, M., Tomiczek, T., Cox, D.T., Lomonaco, P. (2024). Quantifying overtopping performance of green-gray hybrid infrastructure. *Proceedings of the 9th International Conference on Physical Modelling in Coastal Engineering (Coastlab24)*. Delft, Netherlands, May 13-16, 2024.

Menéndez, P., Losada, I.J., Torres-Ortega, S. et al. (2020). The Global Flood Protection Benefits of Mangroves. *Sci Rep* 10, 4404 (2020). doi: 10.1038/s41598-020-61136-6

Ostrow K, Guannel G, Biondi EL, Cox DT and Tomiczek T. (2022) State of the practice and engineering framework for using emergent vegetation in coastal infrastructure. *Front. Built Environ.* 8:923965. doi: 10.3389/fbuil.2022.923965

Ostrow, K. (2023). Performance-Based Design Methodology for Using Emergent Vegetation to Mitigate Wave Overtopping. MS Thesis, Oregon State University, Corvallis.

Verhagen, H., & Loi, T. T. (2012, February). The use of mangroves in coastal protection. In *The 8th International Conference on Coastal and Port Engineering in Developing Countries (COPEDEC) India* (pp. 20-24).

Verhagen, H. J. (2018). The beneficial effects of mangrove forest to sea defence structures. *Threats to Mangrove Forests: Hazards, Vulnerability, and Management*, 475-495.